Time-Dependent Wave Packet Study of the O + O_2 ($v = 0, j = 0$) Exchange Reaction†

Ka-Lo Yeh, Daiqian Xie, and Dong H. Zhang*

Department of Computational Science The National University of Singapore, Singapore 119260

Soo-Y Lee

Department of Chemistry The National University of Singapore, Singapore 119260

Reinhard Schinke

Max-Planck-Institut für Strömungsforschung, D-37073 Göttingen, Germany

Received: February 24, 2003; In Final Form: June 13, 2003

Time-dependent wave packet calculations were carried out to study the O + O_2 ($v = 0$, $j = 0$) exchange reaction on the Siebert−Schinke−Bitterova potential energy surface. Because of the presence of a deep well supporting quasistable ozone complexes, it is found that one needs to propagate wave packets up to 20 ps of time to fully converge the pronounced resonance structures in the total reaction probabilities. We calculated the total reaction probability for total angular momentum $J = 0$ for collision energies up to 0.6 eV, and the integral cross section for collision energies up to 0.4 eV under the centrifugal-sudden approximation. To assess the accuracy of the CS approximation for the reaction, we calculated fully converged cross sections up to a collision energy of 0.04 eV. It is found that (a) both fully converged and centrifugal-sudden cross sections are full of a resonance structure, although not as pronounced as for the $J = 0$ reaction probability, and (b) the centrifugal-sudden approximation can only be used to accurately calculate the thermal rate constant for the reaction, but not the integral cross section.

1. Introduction

It has long been recognized that wave packets, corresponding to a superposition of states of various total energies, provide the most general approach to the solution of the time-dependent Schrödinger equation. However, the time-dependent wave packet (TDWP) method became a powerful tool for quantum reactive scattering problems only after Kouri and co-workers[1,2] demonstrated how to extract S-matrix elements over a wide range of energies from a single wave packet propagation. Since then, the TDWP method has been the driving force for the advancement of quantum scattering studies of chemical reactions, in particular for four-atom reaction systems. The development of the TDWP method made it possible for us (a) to calculate exact total reaction probabilities[4−6] and state-to-state reaction probabilities[7,8] for total angular momentum $J = 0$, as well as fully converged integral cross sections[9,10] for four-atom reactions in full dimension, (b) to study a chemical reaction with two reactive bonds included in full dimension,[11] and very recently (c) to calculate state-to-state integral cross sections for the H + H_2O reaction in five dimensions.[12] In this paper, we report a TDWP calculation for the O + O_2 exchange reaction, which involves long-lived resonances due to a deep well supporting quasistable ozone complexes. To resolve long-lived resonance structures, one has to calculate the reaction probability at thousands of energies, which makes the TDWP method an ideal approach to employ.

Although present only as a trace constituent, ozone plays a crucial role in the absorption of radiation and in the energy balance of the atmosphere.[13] The formation of ozone is believed to proceed through an excited O_3^* complex by the energy transfer mechanism

$$O + O_2 \leftrightarrow O_3^*$$

$$O_3^* + M \leftrightarrow O_3 + M \qquad (1)$$

where O_3^* denotes either a vibrationally excited complex or a complex with one of the low lying electronic states being excited. The rate for forming an excited complex in bimolecular collisions as well as the dissociation rate of that complex are crucial to the abundance of ozone. Given the importance of reaction 1, several experiments have been carried out to measure the temperature dependence of the exchange reaction.[14−18] Classical,[19] quasiclassical,[20−26] and hemiquantal[26,27] trajectory calculations have been performed to study the exchange reaction on a number of potential energy surfaces developed through the years.[20,22,24,28]

Recently, Schinke and co-workers[29] constructed an accurate global potential energy surface for the ground electronic state of ozone based on high level ab initio calculations, denoted as Siebert−Schinke−Bitterova (SSB) PES. Bound states calculations performed on the PES for $^{16}O_3$ and other isotopomers revealed excellent agreement between theory and experiment in vibrational energies.[30] One of the key features of the SSB PES is a transition state region with a tiny barrier separating the well region from the product channel. To assess the accuracy of the PES in the transition state region, Schinke and co-workers very recently performed extensive quasiclassical trajectory (QCT) calculations on the SSB PES, as well as on two newly

† Part of the special issue "Donald J. Kouri Festschrift".

* To whom correspondence should be addressed. E-mail: zhangdh@cz3.nus.edu.sg.

10.1021/jp034471u CCC: $25.00
Published on Web 08/06/2003

modified PES which have different barrier heights from the SSB PES.[31,32] It was found that the variation of the exchange reaction cross section with collision energy and the magnitude of the thermal rate constant below room temperature depended drastically on the shape of the potential at intermediate distances. The thermal rate constant obtained on the SSB PES is significantly lower than the accepted experimental value. They also calculated the total exchange reaction probability for $J = 0$ for the collision energy up to about 0.1 eV by using a time-independent quantum reactive scattering method. It was found that the average quantum reaction probability agrees with the QCT probability very well, indicating that the classical cross section and rate constant should approximate the quantum ones reasonably well.

In this study, we used the TDWP method to study the $^{16}O + {}^{16}O_2$ ($v = 0$, $j = 0$) exchange reaction. Specifically, we calculated the total reaction probabilities for J up to 80 under the centrifugal sudden (CS) approximation, which leads to approximate integral cross sections for a collision energy up to 0.4 eV. To assess the accuracy of the CS approximation, we also calculated the total reaction probabilities for J up to 26 with up to 15 K blocks (the projection of the total angular momentum on the body-fixed axis) included and managed to obtain the fully converged cross sections for the title reaction for collision energies up to 0.044 eV. It is worthwhile to point out here that $^{16}O_2$ ($v = 0, j = 0$) actually does not exist in nature because of Bose statistics. However, because it is much more expansive to calculate the integral cross section for the $^{16}O + {}^{16}O_2$ ($v = 0, j = 1$) reaction, we chose to study the initial $j = 0$ state based on the assumption that dynamics for the $j = 1$ initial state should be close to that for the $j = 0$ initial state.

Section 2 outlines the theoretical methodology of the initial state selected wave packet (ISSWP) approach to atom−diatom reactions. We present the results of our calculation in section 3 and examine the accuracy of the CS approximation to the cross sections for the reaction, followed by the conclusion in section 4.

2. Theory

In this section, we briefly outline the time-dependent wave packet (TDWP) method employed to calculate the initial state selected total reaction probability. The reader is referred to refs 33 and 34 for more detailed discussions of the method. The Hamiltonian for the atom−diatom reaction $O + O_2$ in the reactant Jacobi coordinates (R, r, θ) can be written as

$$H = -\frac{\hbar^2}{2\mu_R}\frac{\partial^2}{\partial R^2} - \frac{\hbar^2}{2\mu_r}\frac{\partial^2}{\partial r^2} + \frac{(\boldsymbol{J}-\boldsymbol{j})^2}{2\mu_R R^2} + \frac{\boldsymbol{j}^2}{2\mu_r r^2} + V(R, r, \theta) \tag{2}$$

where μ_R is the reduced mass between O and O_2, μ_r is the reduced mass for O_2, $\boldsymbol{J}$ is the total angular momentum operator, and $\boldsymbol{j}$ is the rotational angular momentum operator of O_2.

The time-dependent wave function is expanded in terms of the translational basis of R, the vibrational basis $\phi_v(r)$, and the BF total angular momentum eigenfunctions $\mathbf{Y}_{jK}^{JM\epsilon}$ as[33]

$$\Psi(\boldsymbol{R}, \boldsymbol{r}, t) = \sum_{n,v,j,K} F_{nvjK}(t) u_n^v(R)\phi_v(r)\mathbf{Y}_{jK}^{JM\epsilon}(\hat{R}, \hat{r}) \tag{3}$$

where u_n^v is the translational basis function for R which is dependent on v as given in ref 5.

The BF total angular momentum bases $\mathbf{Y}_{jK}^{JM\epsilon}(\hat{R}, \hat{r})$ in eq 3 are the eigenfunctions for $\boldsymbol{J}$, $\boldsymbol{j}$, K and the parity operator. They are defined as[33]

$$\mathbf{Y}_{jK}^{JM\epsilon} = (1 + \delta_{K0})^{-1/2}\sqrt{\frac{2J+1}{8\pi}}[D_{KM}^J + \epsilon(-1)^K D_{-KM}^J]y_{jK} \tag{4}$$

where $D_{K,M}^J$ is the Wigner rotation matrix,[35] ϵ is the total parity of the system defined as $\epsilon_0(-1)^J$ with ϵ_0 being the parity of the system, $0 \le K \le \min(J, j)$ is the projection of total angular momentum on the BF axis, and y_{jK} are spherical harmonics. Note that in eq 4 the $K = 0$ block can only appear when $\epsilon = 1$.

As in ref 33, we construct wave packets and propagate them to calculate the reaction probabilities $P_{v_0 j_0 K_0}^{J\epsilon}(E)$ for each product. The integral cross section from a specific initial state j_0 is obtained by summing the reaction probabilities over all partial waves (total angular momentum J)

$$\sigma_{v_0 j_0}(E) = \frac{1}{2j_0+1}\sum_{K_0\epsilon}\left\{\frac{\pi}{k^2}\sum_{J\ge K_0}(2J+1)P_{v_0 j_0 K_0}^{J\epsilon}(E)\right\} \tag{5}$$

where $k = (2\mu E)^{1/2}/\hbar$.

The numerical parameters for the wave packet propagation were as follows: A total of 269 sine functions (among them 58 for the interaction region) were employed for the translational coordinate R in a range of $[2.5,13.0]a_0$. A total of 80 vibrational functions were employed for r in the range of $[1.5,6.0]a_0$ for O_2 in the interaction region. For the rotational basis, we used $j_{max} = 110$. The number of K values used in our calculation for the fully converged cross section depends on J, with the maximum number of 15. For lower J, we propagated the wave packets for 10^6 a.u. of time to converge the low energy reaction probability. For $J > 20$, we propagated the wave packets for a shorter time because the reaction probability in the low energy region is negligible.

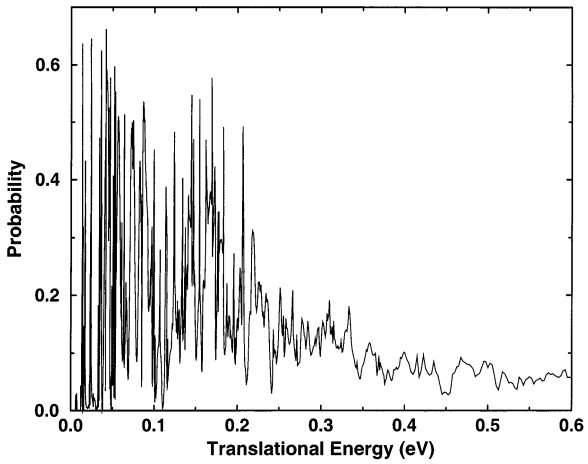

Figure 1. Total reaction probability for the $O + O_2$ ($v = 0$, $j = 0$) exchange reaction on the SSB PES as a function of translational energy for total angular momentum $J = 0$.

3. Results

Figure 1 shows the total reaction probability for the $O + O_2$ ($v = 0$, $j = 0$) reaction on the SSB PES at 1600 energies for collision energy up to 0.6 eV. The probability is dominated by pronounced resonance structures in the low collision energy region, which are due to the trapping of the wave packet inside the potential well. Starting from the collision energy of 0.2 eV, the resonance structures gradually become less pronounced and the overall magnitude of the reaction probability also gradually decreases with further increase of collision energy.

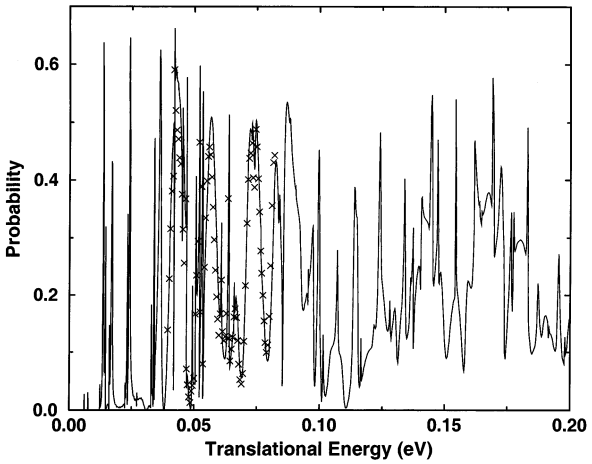

Figure 2. Same as Figure 1 but for the low translational energy. Crosses are the total reaction probabilities calculated by using time-independent (TID) method by Siebert and Schinke,[31] downshifted in energy by 0.0036 eV.

Figure 2 shows the total reaction probability in the low energy region. The probability is very small up to about 0.012 eV, except for two very near resonance peaks at about 0.007 eV, and then rises rapidly together with pronounced resonance structures. There are many resonance peaks with widths of 2−4 cm^{-1}, corresponding to resonance states with lifetimes of 1−2 picoseconds. This is in good agreement with that found in the QCT calculations.[31] The reaction probabilities for most of these pronounced resonance peaks are around 50%. Some are even larger than 60%, close to 2/3. This can happen when energy transfer between the three modes in the system is so complete during the reaction that the three dissociation channels become equal. The crosses shown in the figure are the total reaction probabilities calculated by the time-independent (TID) method of Fleurat-Lessard et al.[31] downshifted in energy by 0.0036 eV. Except for the tiny energy difference which was very likely caused by the difference in defining the asymptotic energy of the SSB potential, the TD probability agrees with the TID result very well.

Total reaction probabilities were calculated under the CS approximation for total angular momentum up to 80. In Figure 3, we show total reaction probabilities for $J = 20$ and 40. Also shown in Figure 3c are the total reaction probability for $J = 0$ together with that for $J = 20$ downshifted in energy by 0.027 eV. As seen, the $J > 0$ CS reaction probabilities behave very similar to the $J = 0$ probability: in the low energy region dominated by pronounced resonances, and relatively smooth in the high energy region. The overall magnitude in the low energy region decreases as J increases. It is found that the reaction probability for J up to 20 resembles the $J = 0$ probability even in the details after a proper shift in collision energy, as shown in Figure 3c. However, the reaction probabilities for larger values of J such as that for $J = 40$ shown in Figure 3b differ substantially in detail from that for $J = 0$.

The CS cross section for the O + O_2 ($v = 0$, $j = 0$) reaction for collision energy up to $E = 0.4$ eV is shown in Figure 4. One striking feature is that the pronounced resonance structures in the total reaction probabilities survive in the cross section. Summing over J, as in eq 5, only partially washes out the resonances. The cross section rises rapidly at $E = 0.012$ eV and reaches the maximum value at a collision energy around 0.11 eV. Then it gradually decreases with the further increase in collision energy.

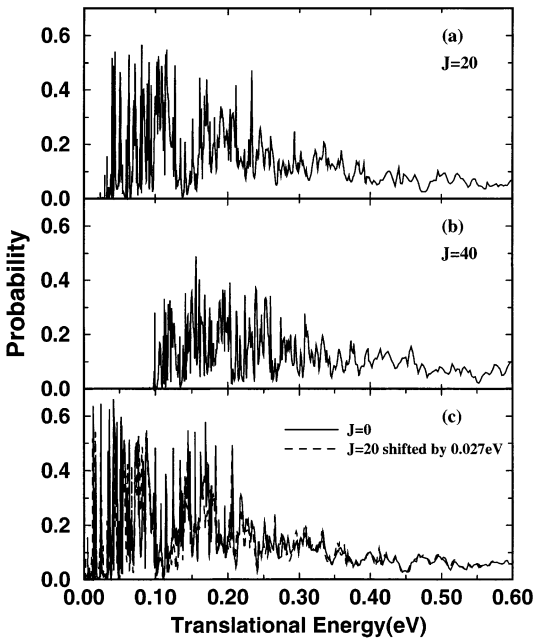

Figure 3. Total reaction probabilities for (a) $J = 20$ (b) $J = 40$ calculated under the CS approximation. (c) The reaction probability for $J = 0$ together with that for $J = 20$ downshifted in energy by 0.027 eV.

To check the accuracy of the CS approximation for the reaction, especially for the resonance structures in the cross section, we calculated the fully converged cross section for collision energy up to 0.044 eV where the CS cross section has pronounced resonance structures as shown in Figure 4. Extensive tests were carried out for $J = 15$, which showed that it is sufficient to use 10 K blocks to obtain fully converged reaction probability for collision energies up to 0.6 eV. Hence we used min(J, 10) K blocks to calculate the total reaction probabilities for J up to 15. We used 12 and 15 K blocks for $16 \leq J \leq 20$ and for $21 \leq J \leq 26$, respectively. The resulting probabilities can be treated as fully coupled-channel (CC) ones. It is computationally demanding to carry out these calculations. It took about 8 days to propagate a wave packet with 10 K-blocks for 10^6 a.u. of time on a dual-processor HP Itanium2 workstation.

In Figure 5, we show the CC reaction probability for $J = 15$ together with the CS one. The $J = 15$ CS probability agrees only qualitatively with the $J = 15$ CC probability. The CC probability has richer, but less pronounced, resonance structures than the CS one, in particular in the low energy region. It can also be seen that the CC probability has a slightly lower threshold energy than the CS one.

In Figure 6, we show the fully converged CC cross section for the reaction for collision energy up to 0.04 eV in comparison with the CS one. The CC cross section is full of resonance structures, although not as pronounced as in the CS cross section, indicating that the pronounced resonance structures in the $J = 0$ total reaction are not washed out completely in the cross section. On average, the CC cross section is larger than the CS cross section, except in the threshold region where they are close to each other. Thus, it is clear that to obtain a quantitatively accurate cross section for this reaction one has to propagate a wave packet for every J with the CC treatment for about 10^6 a.u. of time. As a result, it will be a formidable task even to converge the cross section for very low collision energy as shown here. On the other hand, Figure 6 shows that the QCT cross sections agree with the CC ones extremely well as expected for such a reaction system involving three heavy atoms.

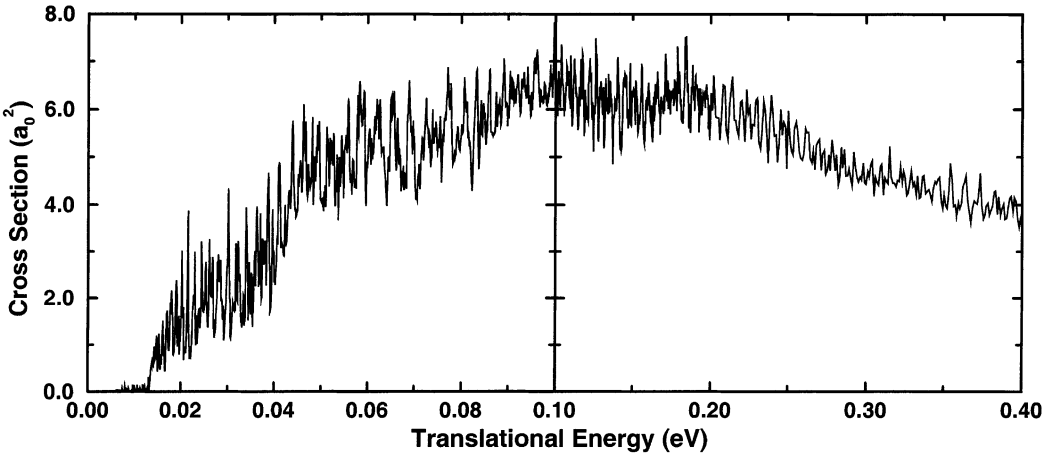

Figure 4. Total cross section for the O + O_2 ($v = 0$, $j = 0$) exchange reaction calculated under the CS approximation.

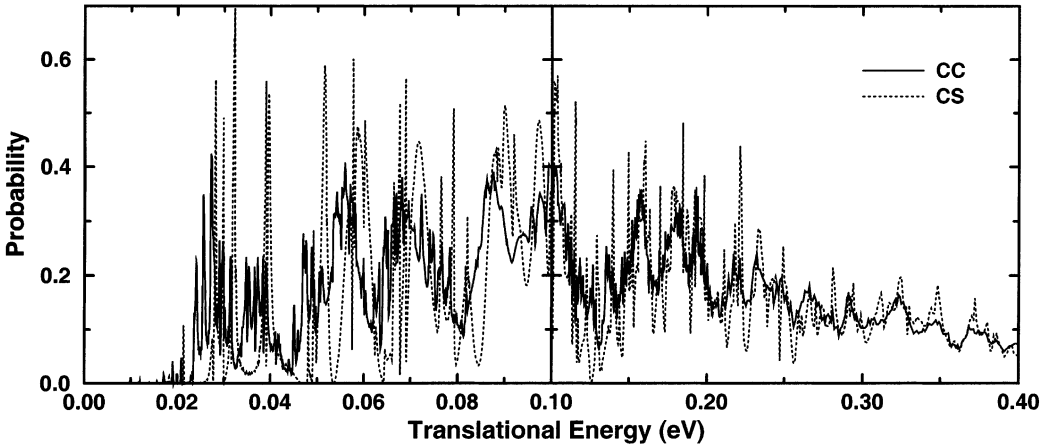

Figure 5. Comparison of the CC reaction probability for $J = 15$ with the CS one.

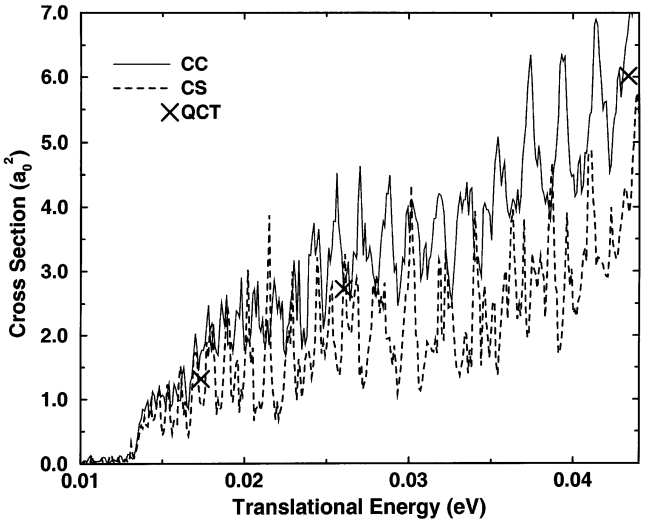

Figure 6. Fully converged cross section for the O + O_2 ($v = 0$, $j = 0$) exchange reaction for collision energy up to 0.044 eV, in comparison with the CS one, and the QCT result of Fleurat-Lessard et al.[31]

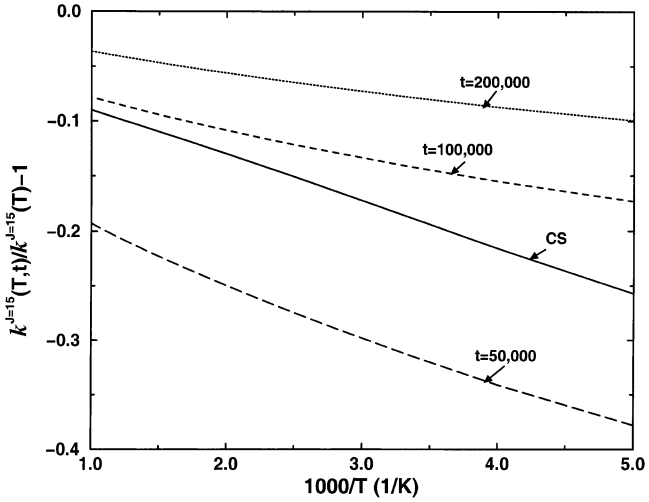

Figure 7. Difference between the contribution of the converged $J = 15$ CC reaction probability to the thermal rate constant, defined in eq 6, and those calculated from $P^{J=15}(t)$ for $t = 50\,000$, $100\,000$, $200\,000$ au of propagation time, as well as that calculated from the $J = 15$ CS reaction probability.

Thus, the QCT method can be a cheap yet sufficiently accurate way to study this reaction.

However, if one is only interested in the thermal rate constant, is it necessary to propagate the wave packet for each J for so such a long time? Let us examine the time convergence of the contribution of $P^J(E, t)$ to the thermal rate constant, defined as

$$k^J(T, t) = \int_0^\infty \mathrm{d}E\, \mathrm{e}^{-E/k_b T} P^J(E, t) \qquad (6)$$

where t is the propagation time, E is the translational energy, and k_b is Boltzmann's constant. We used the CC reaction probability for $J = 15$ shown in Figure 5 to obtain the converged $k^{J=15}(T)$ with respect to propagation time. In Figure 7, we show $k^{J=15}(T, t)/k^{J=15}(T) - 1$ for $t = 50\,000$, $100\,000$, and $200\,000$ au of propagation time. As seen, $k^{J=15}(T, t = 50\,000)$ is about 40 smaller than $k^{J=15}(T)$ at $T = 200$ K, and 20% smaller than $k^{J=15}(T)$ at $T = 1000$ K. The difference is reduced to about 10%

when t is extended to 1000 000−200 000 au. Hence, it is sufficient to propagate wave packets for about 100 000−200 000 a.u. to obtain a well converged thermal rate constant.

Also shown in Figure 7 is the difference between $k^{J=15}(T)$ and $k_{CS}^{J=15}(T)$ which is calculated from the CS probability for $J = 15$. Although the CS reaction probability differs substantially from the CC probability in detail as shown in Figure 5, the contributions from these two probabilities to the thermal rate constant actually agree quite well. Of course, this difference is expected to increase with the increase of J. Because in this temperature region the thermal rate constant is dominated by contributions from the total reaction probabilities for $J = 15-20$, the CS approximation can be used to calculate thermal rate constant for this reaction with a reasonable accuracy.

4. Conclusions

We carried out extensive time-dependent wave packet calculations on the O + O_2 ($v = 0$, $j = 0$) exchange reaction on the SSB PES. Because of the presence of a deep well supporting the stable ozone molecule, it is found that one needs to propagate wave packets up to 10^6 a.u. of time to fully converge the pronounced resonance structures in the total reaction probabilities, and one needs to calculate total reaction probabilities at thousands of energies to fully resolve these pronounced resonance structures.

We calculated the total reaction probability for $J = 0$ for a collision energy up to 0.6 eV, which shows pronounced resonance structures as expected. We also calculated the total reaction probabilities for every J up to 80 by using the CS approximation. It turns out that the partial wave summing only washes out the pronounced resonance structures in the total reaction probability for $J = 0$ partially. The resulting CS cross section is full of pronounced resonance structures.

To assess the accuracy of the CS approximation, we calculated fully converged total reaction probabilities for every J up to 25, which gave rise to the fully converged cross section up to a collision energy of 0.04 eV. It is found that the CC cross section is also full of resonance structures, although not as pronounced as those in the CS cross section. Comparisons made between the CS and CC cross sections cleary indicate that one has to use the CC treatment to obtain quantitatively accurate cross section for the reaction, which has proven to be a formidable task.

However, if one is only interested in the thermal rate constant for this reaction, our calculation shows that it is sufficient to propagate wave packets for 100 000−200 000 au of time, and the CS approximation can also be employed without any significant deterioration in accuracy.

Acknowledgment. This work is supported in part by an academic research grant from Ministry of Education and Agency for Science, Technology and Research, Republic of Singapore.

References and Notes

(1) Mowrey, R. C.; Kouri, D. J. *J. Chem. Phys.* **1986**, *84*, 6466.
(2) Mowrey, R. C.; Bowen, H. F.; Kouri, D. J. *J. Chem. Phys.* **1987**, *86*, 2441.
(3) Zhang, D. H.; Zhang, J. Z. H. *J. Chem. Phys.* **1993**, *99*, 5615.
(4) Neuhauser, D. *J. Chem. Phys.* **1994**, *100*, 9272.
(5) Zhang, D. H.; Zhang, J. Z. H. *J. Chem. Phys.* **1994**, *101*, 1146.
(6) Zhang, D. H.; Light, J. C. *J. Chem. Phys.* **1996**, *104*, 4544.
(7) Zhang, D. H.; Light, J. C. *J. Chem. Phys.* **1996**, *105*, 1291.
(8) Zhu, W.; Dai, J.; Zhang, J. Z. H.; Zhang, D. H. *J. Chem. Phys.* **1996**, *105*, 4881.
(9) Zhang, D. H.; Lee, S. Y. *J. Chem. Phys.* **1999**, *110*, 4435.
(10) Zhang, D. H.; Yang, M.; Lee, S.-Y. *J. Chem. Phys.* **2002**, *117*, 10067.
(11) Zhang, D. H.; Yang, M.; Lee, S.-Y. *Phys. Rev. Lett.* **2002**, *89*, 103201.
(12) Zhang, D. H.; Xie, D.; Yang, M.; Lee, S.-Y. *Phys. Rev. Lett.* **2002**, *89*, 283203.
(13) Wayne, R. P. *Chemistry in Atmospheres*, 2nd ed.; Oxford University Press: Oxford, 1991.
(14) Jaffer, S.; Klein, F. S. *Trans. Faraday Soc.* **1966**, *62*, 3135.
(15) Anderson, S. M.; Klein, F. S.; Kaufman, F. *J. Chem. Phys.* **1985**, *83*, 1648.
(16) Kaye, J. A. *J. Geophys. Res.* **1986**, *91*, 7865.
(17) Larsen, N. W.; Pedersen, T.; Schested, J. *Isotope Effects Gas-Phase Chemistry*; ACS Symp. Ser. 502; American Chemical Society: Washington, DC, 1992; Vol. 11, p 167.
(18) Wiegell, M. R.; Pedersen, N. W. L. T.; Egsgaard, H. *Int. J. Chem. Kinet.* **1997**, *29*, 745.
(19) Stace, A. J.; Murrell, J. N. *J. Chem. Soc., Faraday Trans.* **1978**, *72*, 2182.
(20) Varandas, A. J. C.; Murrell, J. N. *Chem. Phys. Lett.* **1982**, *88*, 1.
(21) Pais, A. A. C. C.; Varandas, A. J. C. *J. Mol. Struct. (THEOCHEM)* **1988**, *166*, 335.
(22) Varandas, A. J. C.; Pais, A. A. C. C. *Mol. Phys.* **1988**, *65*, 843.
(23) Gross, A.; Billing, G. D. *Chem. Phys.* **1993**, *173*, 393.
(24) Gross, A.; Billing, G. D. *Chem. Phys.* **1997**, *217*, 1.
(25) Gross, A.; Billing, G. D. *Chem. Phys.* **1994**, *187*, 329.
(26) Chajia, M.; Jacon, M. *Chem. Phys.* **1995**, *195*, 195.
(27) Chajia, M.; Jacon, M. *J. Chem. Phys.* **1994**, *101*, 271.
(28) Yamashita, K.; Morokuma, K.; Quéré, F. L.; Leforestier, C. *Chem. Phys. Lett.* **1992**, *191*, 515.
(29) Siebert, R.; Schinke, R.; Bittererová, M. *Phys. Chem. Chem. Phys.* **2001**, *3*, 1795.
(30) Siebert, R.; Fleurat-Lessard, P.; Schinke, R.; Bittererová, M.; Farantos, S. C. *J. Chem. Phys.* **2002**, *116*, 9479.
(31) Fleurat-Lessard, P.; Grebenshchikov, S. Y.; Siebert, R.; Schinke, R.; Halberstadt, N. *J. Chem. Phys.* **2002**, *118*, 610.
(32) Hernandez-Lamondeda, R.; Salazar, M. R.; Park, R. T. *Chem. Phys. Lett.* **2002**, *355*, 478.
(33) Zhang, D. H.; Zhang, J. Z. H. *J. Chem. Phys.* **1994**, *101*, 3671.
(34) Zhang, D. H.; Lee, S. Y.; Bear, M. *J. Chem. Phys.* **2000**, *112*, 9802.
(35) Rose, M. E. *Elementary Theory of Angular Momentum*; Wiley: New York, 1957.